SIMULATION OF HYDROGEN SUPPLY IN COUPLED PEM FUEL CELL/LH2 TANK SYSTEMS UNDER AVIATION-RELEVANT CONDITIONS

Bing Ni, Jörg Weiss, Cornelie Bänsch

Deutsches Zentrum für Luft- und Raumfahrt e.V. (DLR), German Aerospace Center, Institute of Engineering Thermodynamics, Energy System Integration, Pfaffenwaldring 38-40, 70569 Stuttgart, Germany

Abstract

Fuel cell-based electric propulsion systems are discussed as one technological option to achieve emission reduction of aviation industry. Especially, for short-haul and regional aircraft applications the feasibility is currently investigated. In this regard, relevant research topics are the upscaling of the polymer electrolyte fuel cell (PEMFC) technology to the megawatt range and the use cryogenic liquid hydrogen (LH2) in order to achieve acceptable energy densities. In this study, the coupling behavior of a multi-modular megawatt PEMFC system with an LH2 tank system is investigated by simulating the subsystems on the basis of a self-developed Modelica model. This PEMFC system, built from a number of individual modules, is designed to deliver the full propulsion power during all phases of the flight. The system concept is to use the heat losses from the fuel cell system for the vaporization and heating of LH2. The supply temperature and pressure of hydrogen under defined control strategies and load profiles are predicted and its effect on the fuel cell performance is investigated. The simulation results indicate that the LH2 tank pressure remains stable during the anode purge process. The LH2 tank pressure changes due to load changes have no significant impact on the fuel cell performance. Furthermore, the hydrogen supply temperature has limited influence on the fuel cell performance and durability within the observed temperature range. Overall, based on the simulation results, no operational restrictions due to pressure and temperature fluctuations in the hydrogen supply from the cryogenic storage system are to be expected.

1. INTRODUCTION

The aviation industry is confronted with a significant challenge regarding decarbonization. Aircraft operations rely on fuels with high energy density to achieve the essential power-to-weight ratio for flight. Concurrently, there is an urgent need for these fuels to minimize harmful emissions, specifically CO_2 and NO_x [1]. Among the various solutions, the application of low-temperature proton exchange membrane fuel cells (LT-PEMFC) in combination with a liquid hydrogen (LH2) tank is a promising technology, that exhibits high volumetric and specific power density and good dynamic behavior [2]. The aircraft 'HY4' has demonstrated the feasibility of liquid hydrogen-based propulsion technology for small aircraft [3,4]. Moreover, using liquid hydrogen as both an energy carrier and a cooling agent for a small aircraft powered by proton exchange membrane fuel cells (PEMFCs) has been investigated by Inacio *et al.* [5]. This study revealed that the cooling capacity of the cryogenic LH2 is insufficient during the cruise phase and an additional liquid cooling system is necessary. For megawatt-range powertrains, a dynamic model was developed in a previous study by the authors [6] to investigate a system design that reuses heat losses from the fuel cell system (FCS) to vaporize and heat LH2 through a thermal system. Extending the research, this study further develops the dynamic model of a multi-modular PEMFC system using a self-developed Modelica model and focuses on investigating the coupling behavior of a multi-modular megawatt PEMFC system with an LH2 tank.

2. METHODS

2.1. System Model

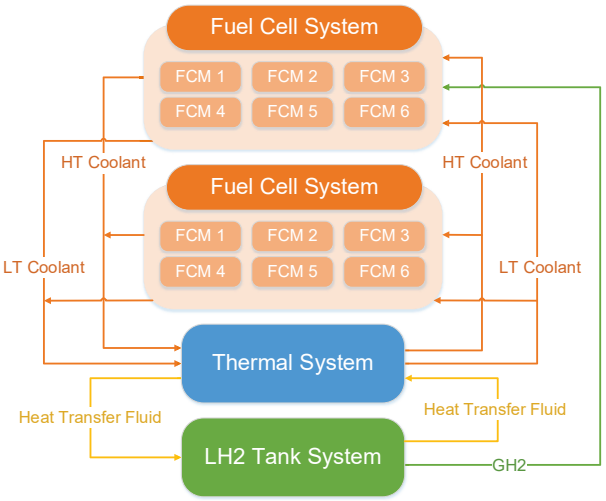

Figure 1 Schematic system overview

The integrated megawatt power system comprises two

doi: 10.25967/630105

multi-modular PEMFC systems, cryogenic LH2 tank system and thermal management system. A schematic overview of system structure is shown in Figure 1. The cryogenic LH2 tank system is designed to store liquid hydrogen at temperatures below the boiling point and precondition LH2 to gaseous hydrogen (GH2). The multi-modular PEMFC systems, configured to deliver megawatt power, is divided into two fuel cell systems (FCS) to investigate various use cases and component interconnections on the electrical side. In consideration of the current development status of LT-PEMFCs, each FCS consists six fuel cell modules (FCMs) and each module delivering approximately 100 kW of maximum power. Due to computational cost, the model considers only half of the MW system, including six FCMs. The FCMs convert chemical energy into electrical energy with an efficiency range of 40% to 60%. The remaining energy is dissipated as heat. To enhance the overall efficiency of the system, the heat loss of FCS is utilized to vaporize and heat up the LH2 via the thermal management system. This thermal management system includes two separate cooling circuits. With the high temperature (HT) cooling circuit the temperature of the fuel cell stacks is managed. The low temperature (LT) cooling circuit regulates the air temperature in the cathode subsystem. The heat transferred out of the FCSs and cathode subsystem by the HT and LT cooling systems is either reused for vaporizing the LH2 via the heat transfer fluid or discharged into the atmosphere.

A description of the basic modelling approach is given in a previous publication [6]. Hence, in the following sections each subsystem is only briefly introduced and the key enhancements introduced to the model are outlined.

2.2. Fuel Cell Module Model

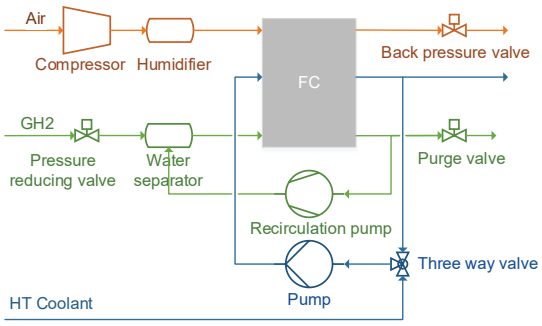

Figure 2 A simplified P&ID of the fuel cell system

The fuel cell module model predicts the fuel cell performance by capturing the transient behaviors of reactant gases regarding temperature, pressure and humidifies under varying operational conditions and load changes. The schematic configuration of the fuel cell system is illustrated in Figure 2. The model of fuel cell stack simulates electrochemical reaction and water transport between the anode and cathode. The ambient air is fed into the cathode subsystem, where it is compressed by an air compressor, then cooled and humidified in the humidifier. It is assumed, that the airflow is sufficiently humidified and adequately temperature-regulated by the LT coolant. The cathode pressure is regulated by means of a cathode back pressure valve with a PI controller. Gaseous hydrogen enters the anode subsystem and pressurized by a pressure control valve to maintain a specific pressure offset between the both sides of the membrane and minimize the risk of gas crossover. In the water separator, the fresh hydrogen is mixed with the recirculated unreacted hydrogen and water. The accumulated liquid water in the anode path is discharged periodically by the purge valve. The nitrogen diffusion from the cathode to the anode is not considered in the model. The HT coolant circuit is configured to maintain the stack temperature in an optimum range.

2.2.1. Fuel Cell Stack Model

According to the defined domains in the Modelica Standard Library, the fuel cell stack model can be categorized into the fluid model, the voltage model and the thermal model. In the fluid model, both the hydrogen flow and air flow are simulated as humid mixtures of ideal gases. The anode, cathode and coolant flow field of the PEMFC stack are treated as lumped volumes respectively, with the spatial variations excluded. The mathematical description of mass flow and pressure losses within the flow field are described in [6].

Voltage Model

The actual fuel cell voltage V_{cell} is obtained by subtracting the overpotentials from the reversible voltage V_{rev}, as shown below [7,8]:

$$V_{cell} = V_{rev} - v_{act} - v_{ohmic} - v_{conc} \quad (1)$$

where v_{act} is the activation overpotential, v_{ohmic} is the ohmic overpotential, and v_{conc} is the concentration overpotential.

The reversible voltage V_{rev} is given by

$$V_{rev} = V_o - \beta(T_{fc} - T_{ref}) + \frac{RT_{fc}}{2F}[ln(\frac{p_{H_2}}{p_{ref}}) + \frac{1}{2}ln(\frac{p_{O_2}}{p_{ref}})] \quad (2)$$

where V_o stands for the standard theoretical cell potential at the reference conditions T_{ref} and p_{ref}, T_{fc}, p_{H_2}, p_{O_2} are the fuel cell operating temperature, the partial pressures of reactant respectively.

The fraction of the reversible voltage, called the activation overpotential, is consumed to drive the electrochemical reaction. Since the reaction at the cathode is significant slower than that at the anode, only the activation overpotential is considered and calculated as follows:

$$v_{act} = \frac{RT_{FC}}{2F\alpha} ln(\frac{i + i_n}{i_0}) \quad (3)$$

where i is the current density, i_0 is the exchange current density, i_n represents the total current density, which combines both the fuel crossover current density and the internal current density, α is the charge transfer coefficient.

The ohmic overpotential, which caused by the electrical resistances of the proton exchange membrane is

determined by

(4) $$v_{ohmic} = i \cdot \frac{d_m}{\delta_m}$$

where d_m is the membrane thickness, δ_m is the membrane conductivity described in [9].

The concentration overpotential, resulting from the reactants concentration change at the electrodes, is calculated by

(5) $$v_{conc} = cln(\frac{i_L}{i_L - i})$$

where i_L is the limiting current density, c is a constant.

All parameters of the voltage model are obtained from the experimental data of the fuel cell stack through curve fitting.

Water Transport Model

The water transport rate N_w is determined by the electro-osmotic water drag from the anode to cathode and the water back diffusion from the cathode to the anode as described below [9]:

(6) $$N_w = \alpha I = n_{drag} \cdot (2I) \cdot \frac{\lambda}{22} - \frac{\rho_{dry}}{M_m} D_\lambda \frac{d\lambda}{dz}$$

where n_{drag} is the electro-osmotic drag coefficient, ρ_{dry} is the membrane density, M_m is the equivalent weight of membrane, λ is the membrane water content and D_λ is the diffusion coefficient, calculated by [10]:

$0 < \lambda < 3$:

(7) $$D_\lambda = 3.1 \cdot 10^{-3} \lambda \left(e^{0.28\lambda} - 1\right) exp\left(\frac{-2436}{T}\right)$$

$3 < \lambda < 17$:

(8) $$D_\lambda = 4.17 \cdot 10^{-4} \lambda \left(161 e^{-\lambda} + 1\right) exp\left(\frac{-2436}{T}\right)$$

In [11], membrane hydration was observed to take approximately 10 seconds, while gas transport occurs within 0.01 to 0.1 seconds. Hence, the time for membrane hydration is considered in this study by using the first order transport function to calculate the membrane water content [9].

2.3. Hydrogen Tank System Model

The LH2 tank system is illustrated in Figure 3. During operation, liquid hydrogen is withdrawn from the LH2 tank by the pressure differences between the tank and the fuel cell system and vaporized and heated in an intermediate circuit, which is initially warmed by a 60-kW electric heater during cold start. The heat transport delay caused by piping in the intermediate circuit is considered.

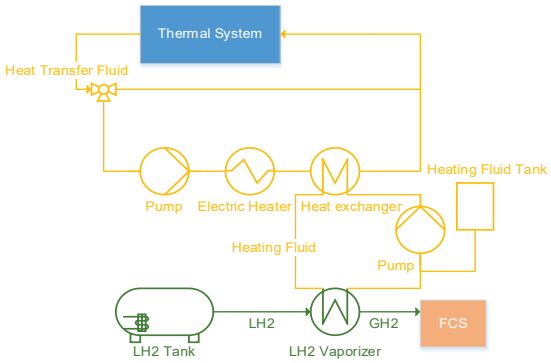

Figure 3 A simplified P&ID of the LH2 tank system

Tank Model

The tank model includes control volumes for the gaseous phase, liquid phase, and the interface between them to simulate dynamic behaviors. The pressure build-up within the tank is achieved by an internal electrical heater. Hence, it is assumed, that the liquid phase is saturated and nucleate boiling occurs directly at the surface of the el. Heater during its operation. The boiling rate $\dot{m}_{boil}$ is calculated by [12]:

(9) $$\dot{m}_{boil} = \frac{\dot{q}_{boil} A_{s,L}}{h_{vap}}$$

where $A_{s,L}$ is the surface area of el. heater, h_{vap} is the heat of vaporization.

3. HYDROGEN SUPPLY CONTROL

During the operation, the pressure in the LH2 tank is maintained at a specified setpoint by the electrical heater and an on-off control strategy with bandwidth of 10 kPa. Once the hydrogen enters the FCM, the hydrogen pressure is adjusted by a pressure reducer valve to track the cathode pressure with a specified offset. The control is accomplished by a PI controller, that uses the measured anode pressure as input and adjusts the valve opening degree as output.

The LH2 is stored in the tank at -245°C. The hydrogen supply temperature before entering the FCM is regulated indirectly through a heat transfer fluid, which is heated by an external electrical heater with on-off control. If the heat transfer fluid's temperature falls below a set threshold, the heater turns on. The hydrogen supply temperature is maintained above the threshold 5°C to prevent water accumulation and freezing in the fuel cell.

4. RESULTS AND DISCUSSION

As input for the simulation a load profile shown in Figure 4 was assumed that represents roughly the different phases of a flight mission. Each load stage represents taxi, take-off, climb, cruise respectively. A first-order transfer function is used to smooth out the transition between different load states. Complete model validation has yet to be accomplished.

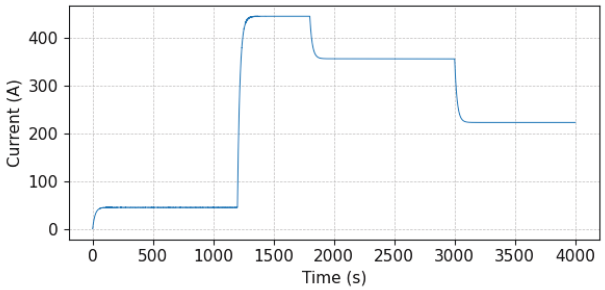

Figure 4 Currents demands for one fuel cell module

Heat Balance

The dissipated and recovered heat in the complete system is illustrated in Figure 5. The total available heat is almost an order of magnitude higher than the consumed heat. Hence, the heat demand for hydrogen evaporation and heating can be covered by the losses of the fuel cell system during operation (after start-up).

During cold start, when the heat transfer medium is not yet sufficiently warm, the electric heater is required to warm up the cooling fluid. The integration of this curve over time yields the total consumed electrical energy, which is approximately 1.4 kWh. It indicates that just a small amount of electrical energy is required for the LH2 vaporization and warm-up at cold-start.

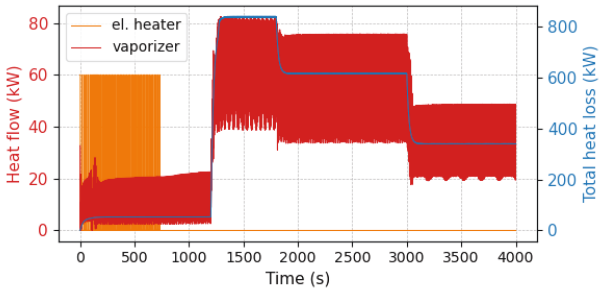

Figure 5 Dissipated and recovered heat of the modeled fuel cell system throughout the flight mission

H_2 Supply Pressure

The variation in tank pressure, the mass flow rate of the LH2 from tank and the corresponding required heat to build up the tank pressure are presented in Figure 6. The tank pressure fluctuates between the predefined setpoints. A sudden increase in LH2 demand during the start-up phase leads to a rapid drop in pressure. When the operation phase shifts from taxiing to take-off phase, more frequent oscillations in the tank pressure occur due to the increased hydrogen demand. An undershoot below the setpoint is not observed. It indicates that the defined heat flow is sufficient to build up the pressure on time during the load change.

In general, the mass flow of hydrogen varies in response to load demand changes and operation phase changes. To prevent the accumulation of nitrogen, the anode is periodically purged with pure hydrogen. Hence, a sudden increase in hydrogen mass flow rate can be observed during each purge period. However, no significant decrease in tank pressure caused by high mass flow rate during the purge it observed. Consequently, anode purging does not significantly affect the tank pressure in the contemplated system according to the simulation results.

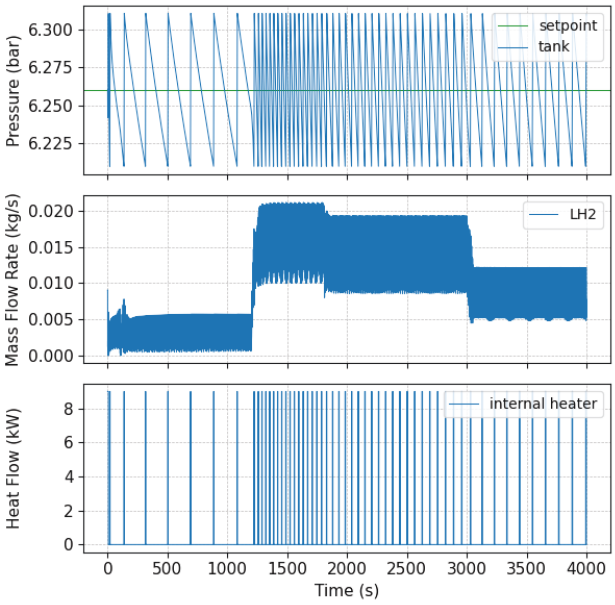

Figure 6 Variation of LH2 tank pressure, LH2 mass flow rate and the heat flow of the internal electric heater throughout the flight mission

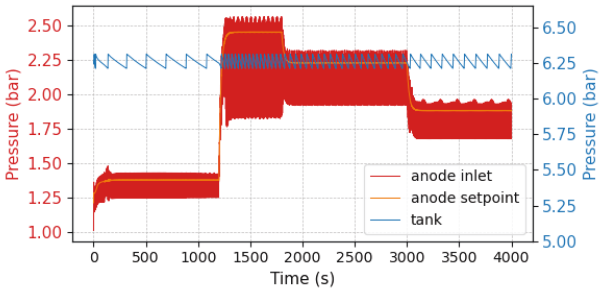

Figure 7 Variation of anode pressure in comparison with the tank pressure throughout the flight mission

In Figure 7 the pressure change in the LH2 tank is compared with the pressure change in the anode of the FCM. No significant correlation is found between the LH2 tank pressure and the anode pressure, either in the steady state or during the load transition due to the different reaction times between the pressure reducer and the tank pressure build-up process. This result confirms that the tank pressure is controlled within a suitable range. The current variations in tank pressure is not found to cause instability in the hydrogen supply.

H_2 Supply Temperature and Humidity: General Observations

In the Figure 8 a), the variation in hydrogen temperature during the flight mission is depicted. The hydrogen supply temperature after the vaporizer, given by the blue curve, is consistently maintained above the threshold of 5°C. It confirms that the setpoint for the heat transfer fluid is defined properly. The sudden increase in hydrogen mass flow rate during purge process causes minor fluctuations in

the hydrogen feed temperature within 0.5°C. This stability indicates that the vaporizer is able to supply sufficient heat and thus is sized properly.

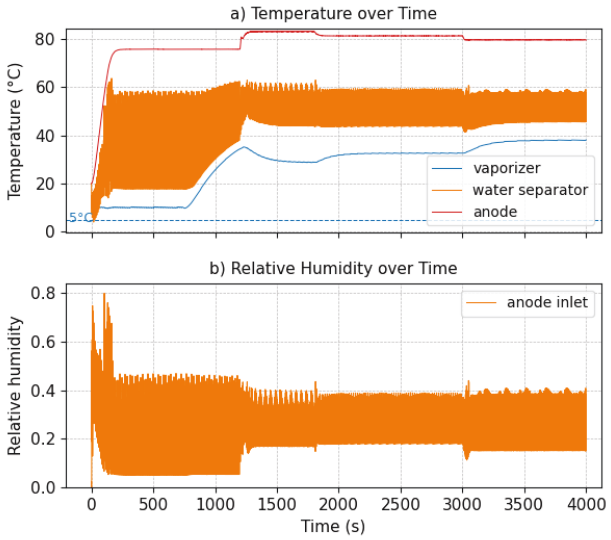

Figure 8 Variation of anode gas temperature and relative humidity at different locations throughout the flight mission

Furthermore, the mixture temperature of the recirculated anode gas and the feed hydrogen in the water separator shown in orange curve in Figure 8 a) varies consistently in a range between 18°C – 62°C. The lowest temperature of mixture, which occurs during purging, tends to follow the changes in the hydrogen feed temperature, since lots of cold hydrogen flows into the fuel cell system. The highest temperature of mixture tends to follow the changes in the anode temperature, since the recirculated warm anode gas contains water vapor, which has a high heat capacity. This unstable mixture temperature at the water separator indicates that the anode inlet gas is humidified at a continuously unstable temperature.

In the Figure 8 b), the orange curve gives the RH of the anode inlet gas, which is determined by the ratio of the partial pressure of water vapor in anode gas mixture to the saturation vapor pressure at the anode temperature. It is assumed, that after entering the anode, the anode inlet gas temperature increases directly to the anode temperature. Flowing the unstable humidification temperature, the RH in the anode inlet gas varies between 0.05 and 0.46 in the taxi phase and between 0.14 -0.39 in the subsequent phases. According to findings in ref. [13], fluctuations in anode RH significantly contribute to the degradation of the membrane electrode assembly (MEA), even when the cathode remains well-humidified. Thus, this unstable RH in the anode inlet gas can negatively affect membrane durability. As a spatially discrete fuel cell performance is not considered in the lumped anode model in this study, it is difficult to observe the impact of RH in the anode inlet gas on the fuel cell performance in the simulation directly. However, considering the findings in ref. [14], which suggest that increasing the RH at the anode inlet from 0.25 to 0.5 can improve the PEMFC performance, there is a potential for further optimization. Therefore, it is recommended to further humidify the anode inlet gas and maintain the RH of the anode inlet gas near 0.5 for a better PEMFC performance and durability.

H_2 Supply Temperature and Humidity During the Taxiing Phase

During the cold start, which is observed in the first 200 s, the anode is cold and warms up to the optimal operating temperature by using the heat loss from the fuel cell. After approximately 780 s, there is a notable increase in the H_2 feed temperature, which can be observed in Figure 8 a). The H_2 feed temperature reaches values of up to 35 °C because the heat demand for evaporating LH2 and heating H_2 is covered by the FCS heat losses. The external electric heater is turned off, since the heat transfer fluid is warm enough. Although the hydrogen feed temperature after the vaporizer and humidification temperature at the water separator increases, the RH at the anode inlet and anode continues to fluctuate in a significant range as before. A possible explanation for this might be that only a minimal amount of liquid water is drained due to the lower humidification temperature before 780s. This amount is so small that even when the humidification temperature increases, the total water content at the water separator does not improve significantly. Therefore, increasing the H_2 temperature during the initial phase does not enhance membrane conductivity significantly.

H2 Supply Temperature and Humidity During the Further Phases

In the further flight phases, the H2 supply temperature and the anode temperature varies within the 12 °C according to the current demand. As the hydrogen demand increases, the H2 supply temperature decreases due to the limited heat supply. In contrast to that, increased power demands cause the anode temperature to rise. The mixture temperature remains within a stable range, as the decrease in H_2 supply temperature is compensated by the increase in anode gas temperature. Hence, the anode inlet gas is humidified within a relatively stable temperature range and its humidity fluctuates within a constant range.

5. CONCLUSIONS AND OUTLOOK

This study investigates the coupling behavior of a multi-modular megawatt PEMFC system with a cryogenic LH2 tank system for aviation applications. The results show that the LH2 tank pressure fluctuates but is maintained above the setpoint during operation by using an internal electrical heater. In addition, the anode purge process does not cause a significant change in the LH2 tank pressure. Due to different reaction times, no significant correlation is observed between tank pressure and anode pressure. Furthermore, under the currently defined control strategies, the hydrogen supply temperature meets the requirement of the PEMFC and shows only minimal influences on the fuel cell performance within the observed temperature range. These results suggest that the proposed system can deliver reliable performance across different phases of flight without operational restrictions caused by fluctuations in hydrogen supply parameters. However, relatively low values and high fluctuations of the relative humidity at the anode inlet between 0.14 and 0.39 have been observed indicating the potential of FCS performance improvements by increasing and stabilizing this value. Further investigations regarding the anode inlet humidity are necessary to evaluate the correlations.

Experimental validation of the obtained simulation results is a key next step to confirm the practical applicability of the system.

ACKNOWLEDGEMENTS

This work was supported by the Federal Ministry of Digital and Transport of Germany as part of the National Hydrogen and Fuel Cell Technology Innovation Program (NIP) (research project BALIS, 03B10705). The funding guideline is coordinated by NOW (National Organization Hydrogen and Fuel Cell Technology) and implemented by Project Management Jülich (PtJ). The responsibility for the content of this publication lies with the authors.

REFERENCES

[1] EUROPEAN COMMISSION. Flightpath 2050: Europe's vision for aviation. LU: Publications Office of the European Union; 2011.

[2] Kazula S, Graaf S de, Enghardt L. Review of fuel cell technologies and evaluation of their potential and challenges for electrified propulsion systems in commercial aviation. J Glob Power Propuls Soc 2023;7:43–57.

[3] Arat HT, Sürer MG. State of art of hydrogen usage as a fuel on aviation. Eur Mech Sci 2017;2:20–30.

[4] Liang S, He L, Wu Y, Zhao H, Li H, Li W. Overview and Analysis of Electric Power Systems for More/All Electric Aircraft. IECON 2023- 49th Annu. Conf. IEEE Ind. Electron. Soc., 2023, p. 1–6.

[5] Inacio G, Mourao C, Castro AL, Lacava P. Feasibility study of using liquid hydrogen tank as energy carriers and cooling agents for a small aircraft powered by PEMFCs, 2022, p. 2022-01–0009.

[6] Ni B, Weiss J, Pracht S, Riedel S, Ansar A, Bänsch C. Dynamic modelling of a megawatt PEM fuel cell system with hydrogen supply from an LH2 tank system. Dtsch Luft- Raumfahrtkongress 2023.

[7] Dicks A, Rand DAJ. Fuel cell systems explained. Third edition. Hoboken, NJ, USA: Wiley; 2018.

[8] Nicolay S, Fritsche L, Lück S, Friedrichs J, Doering R. Development and evaluation of strategies for parallel operation of fuel cell stacks. Dtsch Luft-Raumfahrtkongress 2022:13 pages.

[9] Springer TE, Zawodzinski TA, Gottesfeld S. Polymer Electrolyte Fuel Cell Model. J Electrochem Soc 1991;138:2334–42.

[10] Barbir F. PEM fuel cells. Chapter 4, Elsevier; 2005, p. 73–113.

[11] Wang Y, Wang C-Y. Transient analysis of polymer electrolyte fuel cells. Electrochimica Acta 2005;50:1307–15.

[12] Machalek DM, Anleu GB, Hecht ES. Influence of non-equilibrium conditions on liquid hydrogen storage tank behavior. Int Conf Hydrog Saf 2021.

[13] Vengatesan S, Panha K, Fowler MW, Yuan X-Z, Wang H. Membrane electrode assembly degradation under idle conditions via unsymmetrical reactant relative humidity cycling. J Power Sources 2012;207:101–10.

[14] Zhang L, Liu Y, Bi G, Liu X, Wang L, Wan Y, et al. Modeling and experimental investigation of the anode inlet relative humidity effect on a PEM fuel cell. Energies 2022;15:4532.